Reprinted from June 1984, Vol. 106, Journal of Dynamic Systems, Measurement, and Control

A Calibration and Estimation Filter for Multiply Redundant Measurement Systems

Asok Ray[1]
Mem. ASME.

Mukund Desai

The Charles Stark Draper Laboratory, Inc.,
Cambridge, Mass. 02139

An adaptive filter has been developed for calibration and estimation in multiply redundant measurement systems. The filter is structured in the framework of a fault detection and isolation (FDI) methodology where the decisions are made on the basis of consistencies among all redundant measurements. The consistent measurements are calibrated on-line to compensate for their errors. An estimate of the measured variable is obtained as a weighted average of the calibrated measurements where the individual weights are adaptively updated on-line on the basis of the respective a posteriori probabilities of failure instead of being a priori fixed. The calibration and estimation algorithm is suitable for real-time applications using commercially available microcomputer systems, and has been verified by on-line demonstrations in an operating nuclear reactor.

Introduction

Reliability and performance of complex processes such as spacecraft and nuclear power plants depend upon the validity and accuracy of sensor signals that measure plant operating conditions for information display and control. To enhance safety and plant performance, multiply redundant sensors are often installed for measuring the key variables. In this context, the task of signal validation can be classified into two broad categories: (1) fault detection and isolation (FDI), and (2) measurement calibration and estimation. The objective of this paper is to develop and demonstrate a unified procedure for both aspects of signal validation in multiply redundant measurement systems.

Various methods for fault detection and isolation (FDI) with diverse applications have been reported [1–9]. In this study, an experimentally validated FDI technique [7, 8] has been adopted where the decisions are made on-line from the relative consistencies among all redundant measurements under both steady-state and transient operations; the major assumption is that a measurement is normal if it does not exceed the true value by a specified error bound that can usually be evaluated from the instrument manufacturer's specifications or plant data. The FDI decisions can be made either solely on the basis of current observations or by sequential tests that rely on the past observations as well. The single sample approach is applicable only if the failures to be detected are large in comparison to the measurement noise and uncertainties. A moderate degradation of sensors can be reliably detected and isolated by sequential tests that make use of the cumulative information provided by the measurement history. An on-line calibration and estimation technique has been developed in the framework of the aforesaid FDI methodology via a sequential approach.

For a time-dependent process variable, if the redundant sensors are installed in different spatial locations such as neutron flux detectors in a nuclear reactor, the measurements may exhibit deviations from each other after a length of time even though the sensors are functioning normally. These differences could be caused by time-varying plant parameters, reaction kinetics, transport delay, etc. Consequently, some of the sensors may be erroneously deleted as faulty if they are not periodically recalibrated. On the other hand, failure to isolate a degraded sensor could cause an inaccurate estimate of the measured variable, and the plant performance may be adversely affected if that estimate is used as an input to the controller. For multiply redundant measurements, these problems can be resolved as follows:

(1) All consistent measurements are simultaneously calibrated on-line to compensate for their errors.
(2) The weights of individual measurements for computation of the estimate are adaptively updated on-line on the basis of their respective a posteriori probabilities of failure instead of being a priori fixed.

In the event of abrupt disruptions in some sensor(s) in excess of the specified error bound(s), the respective sensor(s) are isolated by the FDI logic, and only the remaining measurements are calibrated and provide an estimate. If a gradual degradation occurs, the faulty sensor may not be immediately isolated but its influence on the estimate and the calibration of the remaining sensors is diminished as a function of its degradation because its weight decreases with an increase in the a posteriori probability of failure. Thus, if the error bounds of the measurements are appropriately increased to reduce the probability of false alarms, the resulting delay in detecting a gradual degradation could be tolerated because an undetected fault, as a result of the reduced weight, has a little

[1] Currently with GTE Government Systems, 1 Federal Street, Billerica, MA 01821.

Contributed by the Dynamic Systems and Control Division for publication in the JOURNAL OF DYNAMIC SYSTEMS, MEASUREMENT, AND CONTROL. Manuscript received by the Dynamic Systems and Control Division, October 6, 1982.

bearing on the accuracy of calibration and estimation. Moreover, since the weight of a gradually degrading measurment for computing the estimate is smoothly reduced, the eventual isolation of the fault does not cause any abrupt change in the estimate. This feature is very desirable in feedback control systems.

Recently, Stanley [9] has demonstrated the application of a fault detection and measurement estimation technique for closed loop control of a chemical plant. This technique relies on both redundant data and a process model to isolate faults and to compensate for bias errors in measurements. It also adaptively updates the variance of measurement noise to obtain weighted least square estimates of plant variables. However, a detailed mathematical treatment of this technique [9] was not presented. The calibration and estimation technique presented in this paper incorporates the aforementioned properties and has the following distinct features:

(1) No model of the physical process is required if sufficient sensor redundancy is available.
(2) Both fault isolation and sensor calibration algorithms are designed using a posteriori probability of failure of individual (redundant) measurements. The computations are made recursively on the basis of the past observations.

A recursive filter has been designed for fault diagnostics, sensor calibration, and measurement estimation, and verified by on-line demonstrations in an operating nuclear reactor. The development of the filter structure, performance considerations, and the experimental results form the main body of the paper. Brief mathematical descriptions of some important concepts are provided in Appendices A and B.

Algorithm Development

Sensor Calibration. A set of l sensors measuring a plant variable is modelled at the kth sample as

$$\underline{m}(k) = [H^*(k) + H(k)]\underline{x}(k) + \underline{b}(k) + \underline{e}(k) \tag{1}$$

where

$\underline{m}$ is $(l \times 1)$ array of sensor outputs
$H^*$is $(l \times n)$ a priori determined scale factor matrix of rank n; l>n,
H is $(l \times n)$ matrix representing scale factor errors,
$\underline{x}$ is $(n \times 1)$ true value of the measured variable,
$\underline{b}$ is $(l \times 1)$ array of bias errors, and
$\underline{e}$ is $(l \times 1)$ array of measurement noise such that $E(\underline{e}) = \underline{0}$ and $E(\underline{e}\underline{e}^T) = R$

The measurement noise covariance matrix $R(k)$ plays an important role in the design of the adaptive filter for both calibration and estimation. Later, it will be shown how $R(k)$ is dynamically evaluated from the past history of calibrated measurements.

For sensor calibration, $l(n+1)$ parameters in scale factor errors $H(k)$ and bias errors $\underline{b}(k)$ may be estimated along with the estimation of the measured variable $\underline{x}(k)$ [10]. In many industrial applications such as chemical plants and electric power plants, process disturbances and sensor degradations often take place quasi-statically over a long period. In that situation, variations in scale factors and bias are not distinguishable; an additive correction which compensates the combined effect of scale factor and bias errors is sufficient for sensor calibration, i.e., we want to obtain an estimate $\hat{\underline{c}}(k)$ where

$$\underline{c}(k) \triangleq H(k)\underline{x}(k) + \underline{b}(k) \tag{2}$$

On the other hand, if the process variables change rapidly, as in the case of orientation of input axes in navigational sensors, individual compensations of scale factors and bias in the sensors are desirable. Therefore, the sensor calibration filter could be designed for (1) computation of the l-dimensional $\hat{\underline{c}}(k)$ under steady state and quasi-steady-state operations, and (2) appropriate distribution of $\hat{\underline{c}}(k)$ into $l(n+1)$ parameters of $\hat{H}(k)$ and $\hat{\underline{b}}(k)$ under transient conditions, as an alternative to the use of an $l(n+1)$-dimensional filter. (The decision whether to estimate $\hat{H}(k)$ and $\hat{\underline{b}}(k)$ from $\hat{\underline{c}}(k)$ or not may be based on an appropriate criterion.) We have designed a calibration filter which is particularly suitable for steady-state and quasi-steady-state operations when the process variables change rather slowly; for extension to transient operations, a procedure for obtaining $\hat{H}(k)$ and $\hat{\underline{b}}(k)$ from $\hat{\underline{c}}(k)$ is outlined in Appendix A. The rest of this section is devoted to the computation of $\hat{\underline{c}}(k)$

The problem of bias estimation has been addressed by several investigators [1, 2, 11]. Friedland [11] treated the bias as an unknown constant parameter and simultaneously obtained the estimates of bias and physical state variables from the state and measurement equations. Willsky and Jones [2] devised an adaptive filtering system for detection and estimation of abrupt changes in bias (that may occur at an unknown time) using the generalized likelihood ratio (GLR) approach. The adaptive filtering technique, presented in this paper, takes advantage of redundant measurements of a physical variable, and takes into account both gradual and abrupt changes in measurements for calibration and fault detection. As discussed in the previous section, an abrupt disruption in a measurement in excess of a specified bound is isolated by the FDI logic and consequently, the calibration filter is driven by the remaining redundant measurements. In this approach, the additive correction $\underline{c}(k)$ in (2) is treated as a stochastic process (with assumed noise statistics), not as an unknown constant parameter [11]. Furthermore, due to availability of redundant measurements, the computation of $\hat{\underline{c}}(k)$ is independent of that of $\hat{\underline{x}}(k)$, the estimate of the physical variable, thereby eliminating the need for a dynamic process model involving $\underline{x}(k)$. Thus, the scale factor and bia. errors in (2) are modelled together as a discrete-time Markov process.

$$\underline{c}(k+1) = F(k)\underline{c}(k) + \underline{v}(k) \tag{3}$$

where $F(k)$ is the state transition matrix, and $\underline{v}(k)$ is the noise associated with modelling uncertainties such that $E[\underline{v}(k)] = \underline{0}$ and $E[\underline{v}(k)\ \underline{v}(k)^T] = Q(k)$. In the absence of a priori information on bias and scale factor errors of individual measurements in (1), each component of $c(k)$ in (3) are assumed to have identical dynamics, i.e., the state transition matrix $F(k) = \phi(k)I_l$ (for a scalar ϕ). The criteria for selection of the parameters $Q(K)$ and $\phi(k)$ are presented later.

Upon evaluation of $\hat{\underline{c}}(k)$, the estimate for combined effect of bias and scale factor errors, the measurements are simultaneously calibrated at every sample as

$$\underline{y}(k) \triangleq \underline{m}(k) - \hat{\underline{c}}(k) \tag{4}$$

A sensor is assumed to be functioning normally if its calibrated output does not exceed a specified error bound. In this structure, FDI decisions [7, 8] are made on the basis of mutual consistencies among the calibrated measurements with respect to their individual error bounds such that occurrence of false alarms due to scale factor and bias errors are reduced. In the event of a gradual degradation, the calibration correction $\hat{\underline{c}}(k)$ may tend to track the failure. Therefore, the FDI system must be designed to guard against such a situation. This feature is addressed later.

An estimate $\hat{\underline{x}}(k)$ of the measured variable is obtained as a weighted average of those measurements which are determined to be mutually consistent by the FDI logic. We will first obtain $\hat{\underline{x}}(k)$ as a weighted average of the uncalibrated

measurements and later show that this estimate is identically equal to that obtained from the calibrated measurements using the same weighting matrix. Normalizing (1) with respect to $R(k)^{-1/2}$ and denoting $\bar{@}(k) = R(k)^{-1/2}\,@(k)$ yield

$$\underline{\tilde{m}}(k) = \tilde{H}^*(k)\underline{x}(k) + \underline{\tilde{c}}(k) + \underline{\tilde{e}}(k) \tag{5}$$

such that $E[\underline{\tilde{e}}(k)\,\underline{\tilde{e}}(k)^T] = I_l$. A least-square estimate of the measured variable is generated from (5) as

$$\begin{aligned}\underline{\hat{x}}(k) &= [\tilde{H}^*(k)^T\tilde{H}^*(k)]^{-1}\tilde{H}^*(k)^T\underline{\tilde{m}}(k)\\ &= [H^*(k)^TR(k)^{-1}H^*(k)]^{-1}H^*(k)^TR(k)^{-1}\underline{m}(k)\end{aligned} \tag{6}$$

It is important to note that $R(k)$ is adaptively updated, as shown later, so that a degraded measurement, not isolated as faulty, bears a relatively less weight on $\underline{\hat{x}}(k)$.

The residuals of the uncalibrated measurements, defined as $\underline{\tilde{\mu}}(k) \triangleq \underline{\tilde{m}}(k) - \tilde{H}^*(k)\,\underline{\hat{x}}(k)$, can be treated as measurements for the additive correction $\underline{c}(k)$ which we want to estimate for calibration. From (5) and (6), it follows that

$$\underline{\tilde{\mu}}(k) = [I_l - \tilde{H}^*(k)(\tilde{H}^*(k)^T\tilde{H}^*(k))^{-1}\tilde{H}^*(k)^T](\underline{\tilde{c}}(k) + \underline{\tilde{e}}(k)) \tag{7}$$

Since the objective is to calibrate each measurement with respect to the remaining redundant measurements, thereby making the calibration process independent of $\underline{x}(k)$, it appears that the residuals $\underline{\tilde{\mu}}(k)$ can be used to drive the calibration filter. However, it follows from (7) that only $(l-n)$ components of the vector $\underline{\tilde{\mu}}(k)$ are linearly independent; the use of a subset of $(l-n)$ independent components or any linear combinations thereof as the input to calibration filter will yield only partial observability, not complete observability [12, 13], of the state variables $\underline{c}(k)$ in (3) for $F(k) = \phi(k)I_l$. Therefore, the filter must be constructed in an appropriate $(l-n)$-dimensional subspace of R^l such that the projection of $\underline{\tilde{c}}(k)$ onto that subspace is observable from that of $\underline{\tilde{\mu}}(k)$. The projection of $\underline{\tilde{\mu}}(k)$ onto the left null space of $\tilde{H}^*(k)$, known as the parity space [14], is given as

$$\underline{p}(k) = V(k)\,\underline{\tilde{\mu}}(k) \tag{8}$$

and forms a set of $(l-n)$ independent measurements. The $(l-n)\times l$ projection matrix $V(k)$ satisfies the property $V(k)\tilde{H}^*(k) = 0$. Additionally, $V(k)$ is chosen such that its $(l-n)$ rows from an orthonormal basis for the parity space, i.e.,

$$V(k)\,V(k)^T = I_{l-n} \tag{9}$$

With the above choice, it follows that

$$V(k)^TV(k) = I_l - \tilde{H}^*(k)[\tilde{H}^*(k)^T\tilde{H}^*(k)]^{-1}\tilde{H}^*(k)^T \tag{10}$$

and, therefore, the residuals $\underline{\tilde{\mu}}(k)$ in (7) may be expressed as

$$\underline{\tilde{\mu}}(k) = V(k)^TV(k)\,\underline{\tilde{m}}(k) \tag{11}$$

Using the property (9) and the relationship (11), the projection $\underline{p}$ in (8), also known as the parity vector, may be expressed as

$$\underline{p}(k) = V(k)\underline{\tilde{m}}(k) = \underline{\beta}(k) + \underline{\epsilon}(k) \tag{12}$$

where $\underline{\beta}(k) \triangleq V(k)\underline{\tilde{c}}(k)$ and $\underline{\epsilon}(k) = V(k)\underline{\tilde{e}}(k)$. Therefore, it follows from (5) that $E(\underline{\epsilon}(k)) = \underline{0}$ and $E[\underline{\epsilon}(k)\underline{\epsilon}(k)^T] = I_{l-n}$.

To design the calibration filter, (3) is normalized w.r.t. $R(k)^{-1/2}$ and, by projection onto the parity space, the combined effect of scale factor and bias errors is expressed as

$$\underline{\beta}(k+1) = \Phi(k)\underline{\beta}(k) + \underline{\nu}(k) \tag{13}$$

where $\Phi(k) \triangleq \phi(k)I_{l-n}$, and $\underline{\nu}(k) \triangleq V(k)R(k)^{-1/2}\upsilon(k)$, i.e., $E(\underline{\nu}(k)) = \underline{0}$ and $\Theta(k) \triangleq E[\underline{\nu}(k)\underline{\nu}(k)^T] = V(k)R(k)^{-1/2}Q(k)R(k)^{-1/2}V(k)^T$.

Combining the state equation (13) with the associated measurement equation (12), and assuming that the noises $\underline{\epsilon}$ and $\underline{\nu}$ are white and mutually uncorrelated, the standard recursive relations for a Kalman filter [12, 13] are

$$\underline{\hat{\beta}}(k+1) = \phi(k)[\underline{\hat{\beta}}(k) + \Gamma(k)(p(k) - \underline{\hat{\beta}}(k))] \tag{14}$$

where $\underline{\hat{\beta}}(k)$ is the predicted estimator of $\underline{\beta}(k)$ and the filter gain matrix is obtained as

$$\begin{aligned}\Gamma(k) &= \Pi(k)[\Pi(k) + I_{l-n}]^{-1}\\ \Pi(k+1) &= (\phi(k))^2[I_{l-n} - \Gamma(k)]\Pi(k) + \Theta(k)\end{aligned} \tag{15}$$

From the $(l-n)$-dimensional vector $\underline{\hat{\beta}}(k)$, an l-dimensional correction vector $\underline{\hat{\tilde{c}}}(k)$ can be obtained by minimization of a weighted norm $\|\underline{\hat{\tilde{c}}}(k)\|_{W(k)}$ with the relationship $\underline{\hat{\beta}}(k) = V(k)\,\underline{\hat{\tilde{c}}}(k)$ as a constraint [13]. The result, for a positive definite $W(k)$, is

$$\underline{\hat{\tilde{c}}}(k) = W(k)^{-1}V(k)^T[V(k)W(k)^{-1}V(k)^T]^{-1}\underline{\hat{\beta}}(k) \tag{16}$$

Selection of the time-dependent weighting matrix $W(k)$ is a subject of further research and has not been addressed in this paper. Setting $W(k) = I_l$ for all k and using (9), (16) reduces to

$$\underline{\hat{\tilde{c}}}(k) = V(k)^T\underline{\hat{\beta}}(k) \tag{17}$$

Minimization of $\|\underline{\hat{\tilde{c}}}(k)\|$ implies that corrections of least magnitude are applied to calibrate the sensors at every sampling instant although $\underline{\hat{\tilde{c}}}(k)$ may not be an unbiased estimate of $\underline{\tilde{c}}(k)$.

It follows from (17) and (9) that

$$\|\underline{\hat{\tilde{c}}}(k)\| = \|\underline{\hat{\beta}}(k)\| \text{ for all } k \tag{18}$$

and the filter equation (14) can be expressed as

$$\underline{\hat{\beta}}(k+1) = \phi(k)[\underline{\hat{\beta}}(k) + \Gamma(k)V(k)(\underline{\tilde{m}}(k) - \underline{\hat{\tilde{c}}}(k))] \tag{19}$$

An important feature of the calibration filter is that the estimate $\underline{\hat{x}}(k)$ in (6) using the uncalibrated measurements $\underline{\tilde{m}}(k)$ is identically equal to that obtained from the calibrated measurements $\underline{\tilde{y}}(k) = \underline{\tilde{m}}(k) - \underline{\hat{\tilde{c}}}(k)$ in (4). (It can be readily verified using the property $V(k)\tilde{H}^*(k) = 0$.)

In view of (11), defining the residuals of the calibrated measurements as $\underline{\tilde{\gamma}}(k) \triangleq V(k)^TV(k)\,\underline{\tilde{y}}(k)$ and noting that $V(k)^TV(k)\,\underline{\hat{\tilde{c}}}(k) = \underline{\hat{\tilde{c}}}(k)$, the calibration filter in (19) may also be expressed as

$$\underline{\hat{\beta}}(k+1) = \phi(k)[\underline{\hat{\beta}}(k) + \Gamma(k)V(k)\underline{\tilde{\gamma}}(k)] \tag{20}$$

in terms of the residuals of the calibrated measurements. The additive corrections required in (4) may now be obtained as

$$\underline{\hat{c}}(k) = R(k)^{1/2}V(k)^T\underline{\hat{\beta}}(k).$$

Degradation Monitoring and Adjustment of Filter Parameters. The measurement noise covariance matrix $R(k)$ influences both calibration and estimation. Since the accuracy of a measurement is directly related to its variance, $R(k)$ is adaptively updated on the basis of relative performances of the calibrated measurements (that are determined to be consistent by the FDI logic) as

$$R(k+1) = \text{Diag}[f(\pi_i(k))] \tag{21}$$

where $\pi_i(k)$ is the a posteriori probability of failure of the ith measurement and $f(*)$ is an appropriate monotonically increasing function such that $f(*) \to \infty$ as $* \to 1$. The selection of the function $f(*)$ is a design feature; a typical choice, used in the reported experimentation, is $f(*) = 1/(1-*)$.

The calibrated residuals $\underline{\gamma}(k)$ represent a measure of relative degradation of individual measurements. For example, under normal operations, $\|\underline{\gamma}(k)\| \approx 0$ but this may not be true for the uncalibrated residuals $\underline{\mu}(k)$. Whereas abrupt disruptions in excess of the allowable bounds are isolated by the FDI logic, the smaller errors that are not detected by the FDI logic can usually be realized from the a posteriori probability of failure $\pi_i(k)$. Therefore, $\pi_i(k)$ is

recursively computed from the history of the residual γ_i of the ith calibrated measurement on the basis of the following trinary hypotheses:

^0H_i: Normal behavior with density function $^0p_i(\cdot)$

^1H_i: High (positive) failure with density function $^1p_i(\cdot)$

^2H_i: Low (negative failure with density function $^2p_i(\cdot)$

The three density functions for each residual are determined a priori from experimental data and the instrument manufacturers' specifications. Only one test is needed for each residual in the trinary hypotheses approach as compared to the usual binary hypotheses that require two tests to accommodate for positive and negative failures.

Following the recursive relations derived in Appendix B, π_i is obtained as

$$\pi_i(k) = \frac{\psi_i(k)}{1+\psi_i(k)} \tag{22}$$

where

$$\psi_i(k) = \left[\frac{p_i+\psi_i(k-1)}{2(1-p_i)}\right]\left[\frac{^1p_i(\gamma_i(k))+^2p_i(\gamma_i(k))}{^0p_i(\gamma_i(k))}\right]$$

and p_i is the a priori probability of failure of the ith sensor between any two consecutive samples. Therefore, the lower limit of π_i can be set to p_i. On the other hand, solution of (22) shows that, for a gradual degradation of the ith sensor, π_i may asumptotically approach 1 and consequently its variance r_i approaches infinity, i.e., its weight r_i^{-1} approaches 0. To allow a restoration of the sensor following a recovery, the lower limit of the weight r_i^{-1} is set to a small positive value, i.e., the upper limit of π_i is set to $1 - \alpha_i$ where $0 < \alpha_i << 1$ is a design parameter. Therefore, from (22), ψ_i is constrained to have the lower and upper limits of $p_i/(1 - p_i)$ and $(1 - \alpha_i)/\alpha_i$, respectively.

It follows from (13) and (15) that $R(k)^{-1/2}Q(k)R(k)^{-1/2}$ is a critical filter parameter, not $Q(k)$, the covariance matrix for modeling uncertainties in (3). In the absence of appropriate a priori information, the choice of $Q(k)$ with respect to $R(k)$ is a design feature. The steady-state filter gain increases with a larger choice of Q and vice versa. Typically, $Q(k)$ can be selected as a constant matrix equal to the normal steady-state value of $R(k)$ when all measurements are properly calibrated, i.e., $\|\bar{\gamma}(k)\| \approx 0$.

The parameter $\phi(k)$ in the state transition matrix in (3) and (13) influences the dynamic response of the calibration filter (see (15) and (20)). Typically, $\phi(k) = 1$ if $\underline{c}(k)$ in (3) are treated as random walk variables. Alternatively, $\phi(k)$ can be chosen in the interval (0,1) to adapt the calibration filter to time-dependent disturbances. On the other hand, it follows from (11), (12), (14), and (17) that when $E[\hat{\underline{c}}(k)]$ is a constant, the steady-state error $E[(\underline{\tilde{\mu}} - \hat{\underline{c}})] = \underline{0}$ for $\phi = 1$ because the calibration filter operates on a "Type 1" system. For $\phi\epsilon(0,1)$, the filter operates on a "Type 0" system and the steady-state error is a monotonically increasing function of $(1 - \phi)$.

Modification of the FDI System

The calibration filter is designed for on-line operations over a prolonged period in conjunction with a FDI system which is capable of detecting abrupt disruptions in excess of specified bounds. Since all (consistent) measurements are simultaneously calibrated at each sample for small errors, and if a continuous degradation, such as a monotonic drift, occurs sufficiently slowly relative to the filter dynamics, the calibration of the good measurements could be influenced by the degraded sensor (which is also corrected), and thus the fault may be disguised. This problem is resolved by augmenting the FDI system (designed earlier for abrupt disruptions) with one or both of the following procedures:

1. Limit Check on Corrections $\hat{\underline{c}}(k)$ by the Calibration Filter. If the undetected error in a sensor causes simultaneous errors in the calibration of all measurements, the filter will generate a correction for each sensor where the magnitude of the correction for the degraded sensor will be the largest. Therefore, a limit check on the magnitude of the correction for each sensor will detect the aforesaid degraded sensor. The bound for the limit check is selected by a tradeoff between the probability of false alrams and the allowable error in the computation of the estimate of the measured variable.

2. Analytic Measurement Supplementing the Sensors. A mathematical model, formulated on the basis of physical relationships among several process variables, may provide an analytically redundant measurement [15] which is independent of the sensor outputs and, therefore, could be used for testing the calibration filter. If the analytic measurement disagrees with the estimate $\underline{\hat{x}}$ (obtained from the calibration filter) in excess of a given bound, then the implication is either the analytic measurement or the estimate $\underline{\hat{x}}$ is faulty. Upon detecting such a fault, the actual cause of the failure can be resolved with the aid of other information that are usually available. This procedure not only detects a possible malfunctioning of the calibration filter but also guards against simultaneous and identical faults of all sensors possibly due to a common cause, known as a common-mode failure.

Application of the Signal Validation Methodology to a Nuclear Reactor

On-line verification of the signal validation methodology was demonstrated in the 5 MWt nuclear reactor, MITR-II, which is operated by the Massachusetts Institute of Technology [16]. MITR-II is heavy-water reflected, light-water moderated and cooled, and its operating principle is similar to that of a PWR plant. The instrumentation used in this research consists of four power sensors, four primary coolant flow sensors, and three measurements of hot leg to cold leg temperature difference. The noise and statistical characteristics of the MITR-II's instrumentation are similar to those in commercial reactors.

The multiply redundant sensors for power, flow, and temperature measurements are validated on-line with the aid of the FDI methodology [7, 8]. In MITR-II, the flow and temperature sensors are stable and do not need on-line calibrations. To compensate for process disturbances that affect the power measurements, and since the reactor power is presently under computer control that uses the feedback of the power estimate at each sample [17], the power sensors are calibrated on-line.

A flow chart for the signal validation scheme of the power sensors is given in Fig. 1 which can be updated to provide for scale factor and bias compensation under transient operations. At each sample, the power measurements are calibrated and an estimate is obtained as a weighted average of the valid measurements. To guard against any possible drifts of the calibration filter, its outputs are tested using an analytic redundancy and via limit checks as discussed earlier. A mathematical model of the primary coolant system that accepts the validated measurements of power and coolant flow estimates as inputs is used to generate an analytic redundancy ΔT^a for the hot leg to cold leg temperature difference [15]. (Please note that the dynamics of reactor power were not represented in the model.) ΔT^a is compared with the estimate $\Delta\hat{T}$ of temperature difference, obtained from the sensor outputs, at every sample. Inconsistency of $\Delta\hat{T}$ and ΔT^a implies possible errors in the power estimate, and an alarm message is generated to notify the reactor operator. This procedure also guards against a common-mode failure that cannot usually be detected from the power or ΔT sensors alone. The other protection against a drift in the calibration

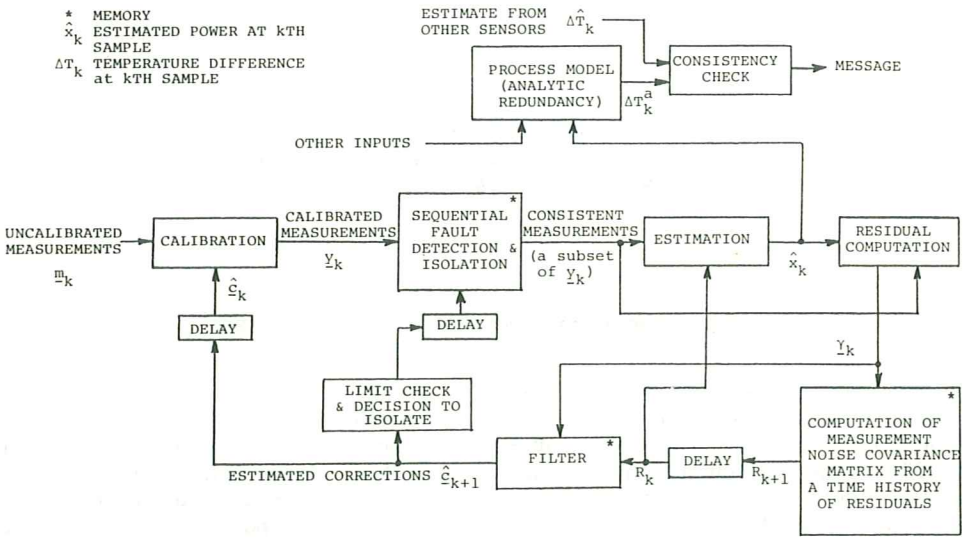

Fig. 1 Flow chart for on-line fault diagnosis and calibration

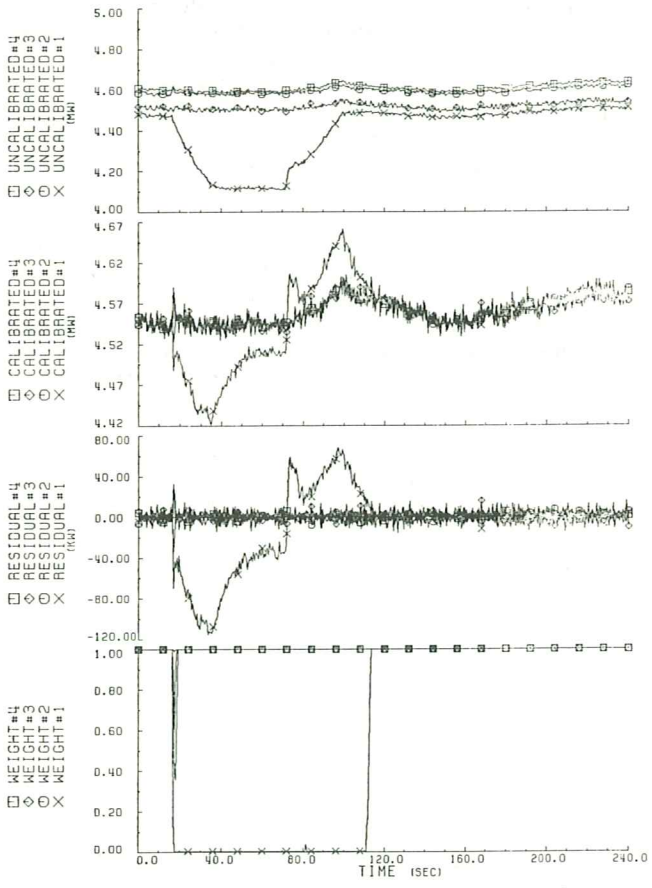

Fig. 2 Uncalibrated and calibrated measurements

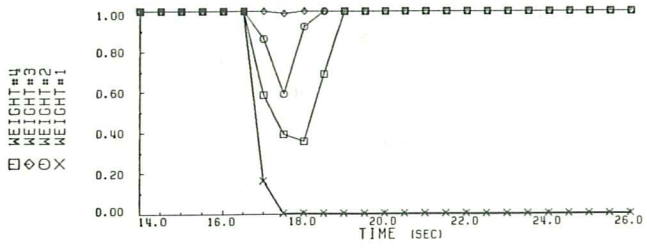

Fig. 3 Weights of calibrated measurements

filter output is provided by testing the additive correction of each measurement. If a specified limit is exceeded, the respective sensor is isolated, and the estimate is obtained from the remaining valid sensors.

The machine executable form of the FDI and calibration code on an LSI-11/23 microcomputer system requires a memory of about 25 kilobytes that include the libraries of FORTRAN and special-purpose real-time routines. The total execution time is less than 150 milliseconds per cycle when no messages are displayed. Therefore, the sampling frequency was selected in the range of 2 hz to 5 hz depending on the volume of messages being displayed. The program has been tested on-line for continuous operations during the last twelve months (except for the weekends when MITR-II is shutdown). During this period, no false alarms were reported when the FDI logic was exercised using the calibrated power measurements. To verify the fault diagnostic capability of the method, different types of sensor failures were simulated while the reactor was in operation. An interesting case is reported below.

To simulate the failure of an electronic component, the scale factor for one of the power sensors was abruptly increased on-line such that it became inconsistent with the remaining three sensors. Thus, the affected sensor was immediately rejected by the calibration filter. Consequently, only the three remaining good measurements were calibrated, and the estimate of power was obtained from these measurements. However, the weight of the affected sensor was reduced to a very small value (because it had a large residual) before it was deleted by the FDI logic. To simulate recovery to the original status following a repair or replacement, the scale factor of the deleted sensor was brought back to its correct value, and the sensor was reactivated on-line by the operator. The reactivated sensor had a correct reading and, therefore, was consistent with the remaining sensors. Initially, this sensor had a small weight, i.e., a large variance in the memory but it gradually recovered to the original status because of a small residual. During the experiment, the estimate of power was unaffected.

A case of sensor calibration in real operations is illustrated in Figs. 2 to 4. As a means of extracting radiation for experiments, MITR-II contains a port of H_2O through the shield. When this port is opened, due to changes in neutron flux profile, the output of power sensor #1 is significantly changed. Since this disturbance occurs slowly (within 18 seconds in contrast to a sampling period of a fraction of a second), the calibration filter generates the correction $\hat{\underline{c}}$ (see Fig. 1) such that all residuals are reduced at each sample. The

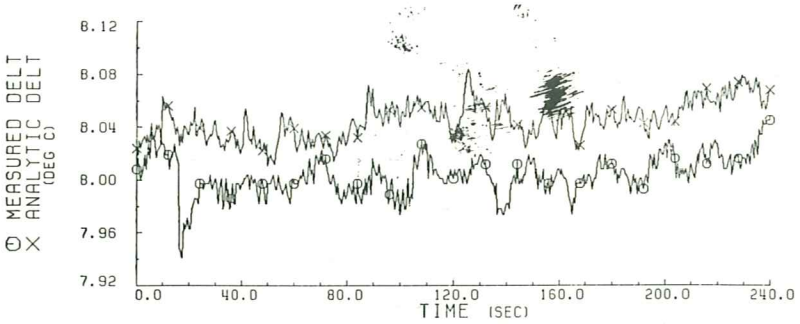

Fig. 4 Comparison of thermal power and estimated power

behavior of all four power sensors are illustrated by a series of curves in Fig. 2. Prior to opening the port at approximately 20 seconds, the uncalibrated measurements had mutual deviations within 120 kW, and the calibrated measurements were clustered together; consequently, the residuals (that are computed on the basis of calibrated measurements) were close to zero, and the relative weights for computing the estimate were identical for all four sensors. On initiation of the disturbance due to opening the port, at the time instant of about 20 seconds, the uncalibrated measurement of sensor #1 gradually decreased from about 4550 kw to 4100 kw within a period of approximately 25 seconds. About 40 seconds later, when the disturbance was removed by closing the port, the uncalibrated measurement reached its original status. During the disturbance, the calibration filter generated the correction $\hat{c}$ such that the deviation of sensor #1 from the remaining sensors did not exceed 125 kw as displayed in the profiles of calibrated measurements and their residuals in Fig. 2.

As the residuals of all measurements increased upon initiation of the disturbance, their relative weights were affected as shown in the last series of cruves in Fig. 2 and in the expanded view of weights during a short period in Fig. 3. Since the residual of sensor #1 remained large for a long period and the remaining sensors recovered rather quickly, only the weight of sensor #1 (that depends upon the time history of its residuals as shown in (21), (22) and Appendix B) was driven to approximately zero. Therefore, the estimated power was practically independent of sensor #1 until the resumption of its normal state. The consistency of the calibrated outputs of sensors #2, #3, and #4 in Fig. 2 shows that the estimated power, obtained as their weighted average, was steady within 50 kw. The small oscillations in power were not the effects of sensor calibration; they resulted from the characteristics of the disturbed process as seen from the identical responses of the uncalibrated outputs of the #2, #3, and #4 sensors in Fig. 2. From Fig. 4, the accuracy of the estimated power can be judged by the close agreement of direct measurement $\Delta\hat{T}$ and analytic measurement ΔT^u of hot leg to cold leg temperature difference, that are indicators of true thermal power and the estimated power, respectively.

For FDI purposes, the error bound of each power sensor was chosen to be 100 kw. Sensor #1 in the uncalibrated system would have been falsely isolated as faulty due to its low value during the disturbance. In the calibrated system, no false alarms occurred becasuse the deviation of sensor #1 relative to any other measurement never exceeded 200 kw, the sum of the specified error bounds of any two measurements under consideration.

Conclusions

For multiply redundant systems, a unified procedure for fault detection and isolation (FDI), sensor calibration, and measurement estimation has been developed and verified by on-line demonstrations in the feedback control of an operating nuclear reactor under both steady-state and transient operations. The FDI decisions are made on the basis of relative consistencies among the calibrated measurements and therefore, are less prone to false alarms. The weights of individual measurements for computing the estimate are not a priori fixed but are updated as an inversely related function of the respective a posteriori probabilities of failure. If the thresholds for individual measurements are increased to reduce the probability of false alarms, the resulting delay in detecting gradual degradations can be tolerated because an undetected fault (within the permissible threshold) does not significantly influence the accuracy of calibration and estimation as the weight of the affected measurement diminishes with its degradation. Moreover, since the weight of a gradually degrading measurement is smoothly reduced, the eventual isolation of the fault does not cause any abrupt change in the estimate; this feature is important for feedback control.

The signal validation methodology can be implemented with the aid of commercially available microcomputers for real-time applications in diverse industrial processes. It is particularly useful for on-line fault diagnosis and calibration of redundant sensors that are installed in different spatial locations such as neutron flux detectors in a nuclear reactor.

References

1 Willsky, A. S., "A Survey of Failure Detection Methods in Dynamic Systems," *Automatica*, Vol. 12, 1976, pp. 601-611.

2 Willsky, A. S., and Jones, H. L., "A Generalized Likelihood Ratio Approach to the Detection and Estimation of Jumps in Linear Systems," *IEEE Trans. on Automatic Control*, Vol. AC-21, Feb. 1976, pp. 108-112.

3 Tylee, J. L., "A Generalized Likelihood Ratio Approach to Detecting and Identifying Failures in Pressurizer Instrumentation," *Nuclear Technology*, Vol. 56, March 1982, pp. 484-492.

4 Clark, R. M., and Campbell, B., "Instrument Fault Detection in Pressurized Water Reactor Instrumentation," *Nuclear Technology*, Vol. 56, Jan. 1982, pp. 23-32.

5 Daly, K. C., Gai, E., and Harrison, J. V., "Generalized Likelihood Test for FDI in Redundant Sensor Configurations," *Journal of Guidance and Control*, Vol. 2, Jan.-Feb. 1979, pp. 9-17.

6 Ray, A., Desai, M., and Deyst, J. J., "Fault Detection and Isolation in a Nuclear Reactor," *Journal of Energy*, Jan./Feb. 1983, pp. 79-85.

7 Desai, M., and Ray, A., "A Fault Detection and Isolation Methodology," *Proceedings of 20th IEEE Conference on Decision and Control*, San Diego, CA, Dec. 1981, pp. 1363-1369.

8 Ray, A., Desai, M., and Deyst, J. J., "On-Line Fault Diagnosis in a Nuclear Reactor by Sequential Testing," *IEEE Transactions on Nuclear Science*, Vol. NS-30, No. 3, June 1983, pp. 1850-1855.

9 Stanley, G. M., "On-Line Data Reconciliation for Process Control," Preprints 1982 Winter Annual Meeting, AIChE, Los Angeles, CA, Nov. 1982, Paper No. 11b.

10 Hall, S. R. et al., "Inflight Parity Vector Compensation for FDI," *Proceedings of National Aerospace and Electronics Conference (NAECON)*, Dayton, Ohio, May 1982, pp. 380-387.

11 Friedland, B., "Treatment Bias in Recursive Filtering," *IEEE Trans. on Automatic Control*, Vol. AC-14, Aug. 1969, pp. 359-367.

12 Gelb, A., ed., *Applied Optimal Estimation*, MIT Press, Cambridge, MA, 1974.

13 Bryson, A. E., and Ho, Y. C., *Applied Optimal Control*, Blaisdell, Waltham, MA, 1969.

14 Potter, J. E., and Suman, M. C., "Thresholdless Redundancy Management with Arrays of Skewed Instruments," *Integrity in Electronic Flight Control Systems*, NATO AGARDOGRAPH-224, 1977, pp. 15-1 to 15-25.

15 Ray, A., et al., "Analytic Redundancy for On-Line Fault Diagnosis in a Nuclear Reactor," *Journal of Energy*, July/Aug. 1983, pp. 367-373.

16 *Reactor Systems Manual*, Report No. MITNRL-004, MIT, Cambridge, MA, 1980.

17 Bernard, J. A., and Ray, A., "Experimental Evaluation of Digital Control Schemes for Nuclear Reactors," *Proceedings of 22nd IEEE Conference on Decision and Control*, San Antonio, Texas, Dec. 1983, pp. 744-751.

18 Athans, M., et al., "The Stochastic Control of the F-8C Aircraft Using a Multiple Model Adaptive Control (MMAC) Method—Part I: Equilibrium Flight," *IEEE Trans. on Automatic Control*, Vol. AC-22, No. 5, Oct. 1977, pp. 769-779.

APPENDIX A

Scale Factor and Bias Compensation

Under transient conditions, to obtain the estimates of scale factor correction $\hat{H}(k)$ and bias $\underline{\hat{b}}(k)$ separately from that of their combined effect $\underline{\hat{c}}(k)$, a procedure (which has not yet been experimentally verified) is suggested.

$\underline{\hat{c}}(k+1)$ and $\underline{\hat{x}}(k)$ are available at the kth sample. This information, along with previously known $\hat{H}(k)$ and $\underline{\hat{b}}(k)$, can be used to predict $\hat{H}(k+1)$ and $\underline{\hat{b}}(k+1)$. The distribution of $\underline{\hat{c}}$ among $\hat{H}$ and $\underline{\hat{b}}$ is achieved using the concept of multiple models [18]. For each sensor, n models are constructed such that only one out of n scale factors is changed in each model to accommodate the correction, and the $(n+1)$st model treats the correction entirely as a bias. For l sensors, the residuals for the $l(n+1)$ models are derived as follows:

$$\gamma_i^j(k+1) \triangleq \hat{c}_i(k+1) = \hat{h}_i^j(k)\hat{x}^j(k) \qquad j=1,2,\ldots,n, \text{ and} \tag{A-1}$$

$$\gamma_i^{(n+1)}(k+1) \triangleq \hat{c}_i(k+1) - \hat{b}_i(k) \qquad i=1,2,\ldots,l$$

where subscripts and superscripts indicate row and column numbers, respectively. The recursive relations for distributions of weights on scale factor components and bias are obtained on a probabilistic basis:

$$w_i^j(k+1) = w_i^j(k)\,p_i(\gamma_i^j(k+1)) \Big/ \left[\sum_{s=1}^{n+1} w_i^s(k)\,p_i^s(\gamma_i^s(k+1))\right] \tag{A-2}$$

with the constraint that

$$\sum_{s=1}^{n+1} w_i^s(k) = 1$$

for every i and every k, where $p_i^j(\cdot)$ is the a priori density function for the residual of the jth model of the ith sensor. The initial conditions for the weights are set such that $w_i^j(0) \geq 0$ and

$$\sum_{j=1}^{n+1} w_i^j(0) = 1$$

for every i, and if the initial calibration of the sensors is correct, then $\hat{b}_i = 0$ and $\hat{h}_i^j = 0$ for every i and j.

The bias and scale factor corrections are predicted as:

$$\hat{b}_i(k+1) = w_i^{(n+1)}(k+1)\hat{c}(k+1) \tag{A-3}$$

$$\hat{h}_i^j(k+1) = \begin{cases} w_i^j(k+1)\hat{c}(k+1)/\hat{x}^j(k) & \text{if } \hat{x}^j(k) \neq 0 \\ \hat{h}_i^j(k) & \text{if } \hat{x}^j(k) = 0 \end{cases}$$

The above relations are equivalent to

$$\underline{\hat{c}}(k) = \hat{H}(k)\underline{\hat{x}}(k-1) + \underline{\hat{b}}(k) \tag{A-4}$$

which is an approximation of (2). However, if the sampling frequency is sufficiently large with respect to the process dynamics, $\underline{\hat{x}}(k)$ should be close to $\underline{\hat{x}}(k-1)$. Another potential source of inaccuracy in the estimation of $\hat{H}(k)$ is the dynamics of calibration filter. Unless the filter response is properly adjusted, changes in $\underline{\hat{c}}(k)$ may be damped, thereby making $\hat{H}(k)$ inaccurate.

APPENDIX B

Recursive Relations for a Posteriori Probabilities in Multiple Hypotheses

Let $z(1), z(2), \ldots, z(k), \ldots$ be (conditionally) independent measurements of a variable at consecutive sampling instants. The $(N+1)$ distinct possible modes of operation are designated as $(N+1)$ mutually exclusive and exhaustive hypotheses.

$^0H(k)$: normal operation at the kth sample

$^iH(k)$: abnormal operation at the kth sample, $i=1,2,\ldots,N$

such that each hypothesis can be treated as a Markov state. The problem is to derive a recursive relation for the a posteriori probability of any abnormal operation

$$\pi(k) = P\left[\bigcup_{i=1}^{N} {}^iH(k) \mid z(1), z(2), \ldots, z(k)\right]$$

based on the measurement history.

Let the probability of transition from one state to another be denoted as $a_{ij}(k) = P[{}^jH(k) \mid {}^iH(k-1)]$ such that

$$\sum_{j=0}^{N} a_{ij}(k) = 1$$

for every i and every k.

Let the joint probability $\xi_i(k) \triangleq P[{}^iH(k), Z(k)]$ where $Z(k)$ denotes the ensemble $\{z(1), z(2), \ldots, z(k)\}$. Then

$$\xi_j(k) = P[{}^jH(k), z(k), Z(k-1)]$$
$$= P[z(k) \mid {}^jH(k)]P[{}^jH(k), Z(k-1)].$$

Since

$$P[{}^jH(k), Z(k-1)] = \sum_{i=0}^{N} P[{}^jH(k),$$

$${}^iH(k-1), Z(k-1)] = \sum_{i=0}^{N} P[Z(k-1) \mid {}^iH(k-1)]$$
$$P[{}^jH(k) \mid {}^iH(k-1)]P[{}^iH(k-1)]$$
$$= \sum_{i=0}^{N} P[{}^jH(k) \mid {}^iH(k-1)]P[{}^iH(k-1), Z(k-1)],$$

it follows that

$$\xi_j(k) = p_j(k) \sum_{i=0}^{N} a_{ij}(k)\,\xi_i(k-1) \tag{B-1}$$

where a priori conditional probability is denoted as $p_j(k) = P[z(k) \mid H_j(k)]$ for every j. The a posteriori probability is defined as

$$\pi_j(k) = P[{}^jH(k) \mid Z(k)] = P[{}^jH(k), Z(k)] \Big/ \left(\sum_{i=0}^{N} P[{}^iH(k), Z(k)]\right)$$
$$= \xi_j(k) \Big/ \left(\xi_0(k) + \sum_{i=1}^{N} (\xi_i(k))\right)$$
$$= \psi_j(k) \Big/ \left(1 + \sum_{i=1}^{N} \psi_i(k)\right) \tag{B-2}$$

where

$\psi_j(k) \triangleq \xi_j(k)/\xi_0(k)$

$$= \frac{p_j(k)}{p_0(k)} \frac{a_{0j}(k) + \sum_{i=1}^{N} a_{ij}(k)\psi_i(k-1)}{a_{00}(k) + \sum_{i=1}^{N} a_{i0}(k)\psi_i(k-1)} \tag{B-3}$$

Then,

$$\pi(k) = P\left[\bigcup_{j=1}^{N} {}^{j}H(k) \mid Z(k)\right] = \sum_{j=1}^{N} \pi_j(k) = \frac{\Psi(k)}{1+\Psi(k)} \tag{B-4}$$

where

$$\Psi(k) \triangleq \sum_{i=1}^{N} \psi_i(k) \tag{B-5}$$

The above expression for $\Psi(k)$ can be expressed by a simple recurrence relation under the following assumptions:

1. No transition from any abnormal mode to the normal mode, i.e., once a measurement has failed, it does not recover unless repaired, i.e., $a_{i0}(k) = 0$ for every $i \neq 0$ and every k.
2. Transition from the normal mode to any abnormal mode is equally likely. If p is the probability of failure during any sampling period, then $a_{0i}(k) = p/N$ and $a_{00}(k) = 1 - p$ for every $i \neq 0$ and every k.
3. Transition from one abnormal mode to any other abnormal mode is equally likely, i.e., a failed measurement may assume any one of the possible N abnormal modes with equal probability, i.e., $a_{ij}(k) = 1/N$ for every $i \neq 0$ and every $j \neq 0$.

Using the above assumptions and (B-5) in (B-3),

$$\psi_j(k) = \frac{p + \sum_{i=1}^{N} \psi_i(k-1)}{N(1-p)} \cdot \frac{p_j(k)}{p_0(k)}$$

$$= \frac{p + \Psi(k-1)}{N(1-p)} \cdot \frac{p_j(k)}{p_0(k)} \tag{B-6}$$

Therefore, combining (B-5) with (B-6) yields the relationship

$$\Psi(k) = \frac{p + \Psi(k-1)}{N(1-p)} \cdot \sum_{j=1}^{N} \frac{p_j(k)}{p_0(k)} \tag{B-7}$$